Ai, Q., Weaver, P. M., & Azarpeyvand, M. (2018). Design and mechanical testing of a variable stiffness morphing trailing edge flap. *Journal of Intelligent Material Systems and Structures*, *29*(4), 669-683. https://doi.org/10.1177/1045389X17721028

Design and mechanical testing of a variable stiffness morphing trailing edge flap

Qing Ai,[1] Paul M.Weaver[1] and Mahdi Azarpeyvand[2]

Abstract

Morphing structures that are both light-weight and conformal to the aerofoil are currently being considered as promising candidates for the next generation of aircraft high-lift systems. Utilizing spatially variable stiffness materials in morphing structures leads to a possible reduction in the actuation energy requirement and also enables geometric control over the deformed shape of the morphing structure, resulting in enhanced aerodynamic and aeroacoustic performance. In this study, a design optimization methodology has been developed to identify the required material stiffness variations of a morphing structure for target optimal deformed shapes. In the optimization scheme, a layer-wise sandwich beam model is used to predict the structural behaviour of the flap with a specific material stiffness variation. Two-dimensional fluid/structure static aeroelastic interaction analysis is performed in the design optimization. Finite element analysis and mechanical tests were also carried out for a chosen optimization result to study the actuation requirements and the capability of control over the deformed shape of the morphing trailing edge. Numerical and experimental results confirm the feasibility of the proposed optimization methodology for identifying the required stiffness variation in the core and also ways of using rapid prototyped honeycomb core to realize the honeycomb core stiffness variations are discussed.

Introduction

Aircraft wing and wind turbine blades are usually optimized for certain operating conditions and, as such, adaptive geometry change capabilities that enable active load control and gust load alleviation could significantly enhance the overall system performance (Ai *et al.,* 2015; Barbarino *et al.,* 2011; Campanile *et al.,* 2004; Lachenal *et al.,* 2013). Morphing structures have received growing interest from the research community as well as aviation, wind energy and automobile industries (Lachenal *et al.,*

[1]Advanced Composites Centre for Innovation and Science (ACCIS), Department of Aerospace Engineering, University of Bristol, Bristol BS8 1TR, UK
[2]Aeroacoustic and Aerodynamic Research Group (A^{2}RG), Department of Mechanical Engineering, University of Bristol,Bristol BS8 1TR,UK
Email: qa12090@bristol.ac.uk

Prepared using sagej.cls *[Version: 2013/07/26 v1.00]*

2013; Chopra 2002; Weisshaar 2013; Barbarino *et al.,* 2011), owing to their excellent performance, light-weight and reduced structural complexity. For example, the need for reduced cost of wind energy has lead to significantly increased wind turbine blade size, which has adversely affected efficiency of traditional control systems using pitching and yawing operations. Active control systems including morphing structures show significant potential for optimizing load distribution along the blade and alleviating gust loads thus leading to an increased fatigue life of the structure and a reduced power cost (Ai *et al.,* 2015; Lachenal *et al.,* 2013; Daynes and Weaver 2012a,b). For aeroplanes, high-lift systems have been widely used on wings to control the lift and drag forces during take-off and landing. However, conventional wing control surfaces including leading edge slats and trailing edge flaps usually use discrete rigid structural components that are mechanically articulated around hinges and linkages to provide the required wing geometry changes, which significantly increases system complexity and the overall structural weight. On the other hand, slat slots and fairings present with the flaps and ailerons have been identified as major sources for airframe noise and drag(Dobrzynski 2010).

Unlike conventional control surfaces, morphing structures typically use structural deformation including bending and twisting to provide the required geometry changes, *i.e.* they remain conformal to the aerofoil. Continuous profile changes and smooth surfaces over the morphing structure significantly reduce drag effects and eliminate cavity/slot type noise, leading to an improved aerodynamic efficiency, control effectiveness and a reduced system complexity (Campanile *et al.,* 2000; Campanile 2007; Daynes and Weaver 2012a; Fischer *et al.,* 2006; Reckzel 2003; Molinari *et al.,* 2016). Furthermore, the flow field including the boundary layer around the aerofoil's trailing edge could be significantly affected by the deformed morphing structures, which leads to a possible mitigation in induced noise levels.

Concepts

In recent decades, promising progress in morphing technologies including new morphing mechanisms and concepts, novel actuation methods and smart materials has been made (Thill *et al.,* 2008; Lachenal *et al.,* 2013; Chopra 2002; Weisshaar 2013; Barbarino *et al.,* 2011). A variety of concepts have been successfully tested at a laboratory level and are described in this section.

Companile *et al.* (2000) developed a Belt-Rib concept which consists of a closed belt and supporting in-plane spokes in the Adaptive Wing project at German Aerospace Centre (DLR). The concept used selectively distributed structural flexibility to produce required geometry changes and the material and structural stiffness distribution can be optimized for specific design and application requirements. Experimental studies successfully confirmed that the Belt-Rib concept could be a feasible solution for aerofoil shape control purposes satisfying the requirements of the geometrical adaptability, the load-carrying ability and light-weight. A further study with the concept has also indicated that by exploiting the aerodynamic and aeroelastic amplification effects of the aerofoil, the actuation requirement of the Belt-Rib could be significantly reduced (Campanile *et al.,* 2004).

A flexible trailing edge control surface was developed and tested by Bartley *et al.* (2004) in the DARPA/AFRL/NASA Smart Wing Program. The morphing trailing edge proposed consisted of three main parts: (1) an elastomeric (silicone) outer skin of large strain capability, (2) a flexible honeycomb core reinforcing the through-thickness direction stiffness of the structure and (3) a center composite leaf spring stabilizing the core and skin. Wind tunnel tests showed that the morphing trailing edge (TE) segment was able to undergo large trailing edge deflection of up to 20°(Bartley *et al.,* 2004). Results also suggested that the actuation requirement can be further reduced by changing the honeycomb core

material from aluminium to a non-metallic material, such as a phenolic or aramid core. Drawing upon this concept, Daynes and Weaver (2012a) constructed a morphing trailing edge device comprising carbon fibre reinforced plastic (CFRP) upper skin, an aramid hexagonal honeycomb core and a silicone lower skin for wind turbine applications. A demonstrator was actuated from -10° to 10° at up to 0.4 Hz by a CFRP push/pull rod using conventional servomotors. Aeroelastic analysis results showed that compared to a hinged flap, the morphing device can produce the same lift change with 30% less tip deflection, which is believed to be due to the differing geometries and tip morphing angles (Daynes and Weaver 2012a,b).

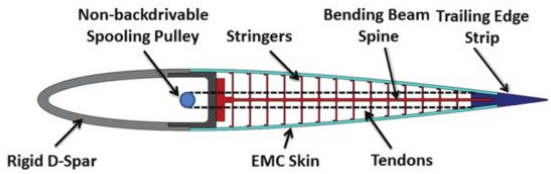

Figure 1. Fish bone active camber morphing structure (Woods *et al.,* 2014)

Inspired by fish bone structures, a morphing structure concept for aerofoil camber changes was developed by Woods *et al.* (2014; 2015). The concept consisted of four primary components: a compliant spine with stringer skeleton, a pre-tensioned elastomeric matrix composite skin, an antagonistic drive with a spooling pulley and a non-morphing stiff main spar (see Figure 1). The morphing structure was actuated by the spooling pulley which drives the tendons to generate a bending moment at the trailing edge to deform the structure. Wind tunnel tests and optimization studies have been carried out with the morphing concept. Experimental results showed that the proposed morphing trailing edge presents several superior properties compared with traditional flaps including considerably higher lift-to-drag ratios.

Corrugated structures have been used in morphing structures (Thill *et al.,* 2008, 2010; Shaw 2015) as well. Yokozeki *et al.* (2014) and Takahashi *et al.* (2016) developed a morphing wing with leading edge and trailing edge made of corrugated structures. The morphing structure was actuated via a pulling wire through the bottom surface of the wing. A hardware demonstrator was built based on the analytical and numerical structural analyses with aerodynamic loads and actuation forces considered. Wind tunnel tests were carried out to assess the aerodynamic performance of the morphing wing and also to measure the deformed shapes of the wing under pressure loads and actuation forces. Experimental results showed that the morphing wing presented superior aerodynamic performance with higher lift coefficients compared to a reference wing using conventional flap due to the seamless deformed shape of the morphing wing. Numerical and experimental studies confirmed the feasibility of the proposed morphing wing concept as an efficient aerofoil control device. However, the flexible wing was actuated through a flexible wire and hence only one-way, in this case downwards deflection of the leading edge and trailing edge were achievable.

Optimization design

Aero-structural optimization studies and aeroelastic analyses of morphing structures have been carried out to investigate the effects of aerodynamic loads on the responses on morphing structures including the effects on the actuation requirements.(De Gaspari *et al.,* 2011; Molinari *et al.,* 2011; Bae *et al.,* 2005; Molinari *et al.,* 2015)

A multi-disciplinary morphing structures design optimization methodology was developed by Monlinari *et al.* (2011) capable of concurrently optimizing aerodynamic and structural parameters from the very beginning of the interactions between aerodynamics, structures and control theory and applied to a morphing structure design case. The optimization method enables assessment of the effects of the strong coupling between the structure and aerodynamic loads. The proposed optimization methodology was then applied to a morphing flap design using dielectric elastomer as actuators. Results show that superior aerodynamic performance can be achieved using this concurrent coupled optimization method compared to the other sequential optimization methods. Aeroelastic analysis of a morphing wing using a model coupling finite element method (FEM), aerodynamic and shape control theory has also been used in the design process of morphing structures (Bae *et al.,* 2005). It is found that the deformed shapes of the adaptive aerofoils can be significantly affected by the pressure loads and the actuation requirement can be reduced by exploiting the aerodynamic effects.

Gaspari *et al.*(2011) proposed a two-level optimization approach to determine the optimal deformed aerofoil shape. The optimization method consisted of two steps: the first step is an optimization approach to select optimal deformed shapes which are used as targets to then identify the topology design of the internal structure in the second optimization step. The developed methodology was applied to the design of a morphing leading edge and a trailing edge. Results showed that it is feasible to design a morphing leading edge with a tailored internal structure set for target deformed shape allowing large deformation capability with appropriate trailing edge modifications made to the designed mechanism.

Variable stiffness materials and structures

Conflicting requirements for load carrying capability, shape adaptability and light weight of morphing structures provide scope of using novel materials including variable stiffness materials (Panesar *et al.,* 2012; Thuwis *et al.,* 2010; Raither *et al.,* 2014; Ai *et al.,* 2015; Kuder *et al.* 2016a,b; Diaconu *et al.* 2008), mostly as skins. Variable stiffness materials refer to materials in which the mechanical properties change as a function of spatial position. A bistable morphing flap concept using composite laminates of variable angle tows was developed and built (Panesar *et al.,* 2012), allowing for the in-plane stiffness tailoring in a single ply and tests with a proof-of-concept demonstrator confirmed the feasibility of the proposed concept.

Variable stiffness skins have been used in the design of a morphing leading edge by Thuwis *et al.* (2010). In the study, the potential of using variable stiffness skins to control the structurally deformed shape of the morphing leading edge was investigated using curvilinear fibre composite material as skins allowing for desirable stiffness variations to match a target optimal shape under actuation forces and pressure loads. Results showed that the design space can be significantly extended by using a variable-stiffness skin and that control over the deformed shape can be achieved. A variable camber aerofoil concept using a variable stiffness skin to change the structural rigidity according to the operational states was proposed by Raither *et al.* (2014) concluding that significantly increased structural efficiency,

reductions in actuation energy and also weight saving can be achieved. In a more recent study, a novel morphing trailing edge design using a honeycomb core of axial variable stiffness was studied. (Ai *et al.,* 2015). These results show that by introducing variable stiffness materials into the morphing structures could affect the actuation energy of the system and also enable tailoring of the morphing profiles, *i.e.* the deformed shape of the morphing trailing edge which significantly affects the aerodynamic and aeroacoustic performance of the aerofoils. Kuder *et al.* (2016a; 2016b) studied the usage of bi-stable laminates embedded in the aerofoil which can be effectively used as a stiffness control switch. With the bi-stable elements, the morphing aerofoils can present two stiffness states: the rigid and soft modes. Furthermore, the actuation requirements can then be significantly reduced using the bistable elements as a stiffness switch for the morphing structure.

This paper presents design, manufacturing and mechanical tests of a morphing trailing edge flap using spatially variable stiffness materials. Of particular interest is the control capability over the deformed shape of the morphing trailing edge by selectively changing the in-plane stiffness variation, which has potential for aerofoil self-noise mitigation effects (Ai *et al.,* 2015, 2016b). An integrated design optimization methodology of a morphing trailing edge using a 3D printed honeycomb core of axial variable stiffness is proposed. As shown in Fig.2, the axial direction of core is selected to align with the chord of the morphing flap. Instead of focusing on increasing the trailing edge deflection capabilities, the proposed design scheme further enhances the control capability over the deformed shape of the morphing trailing edge through utilizing spatially variable stiffness materials. The optimization method proposed identifies the desired axial stiffness variations in the honeycomb core that could provide morphing profiles matching the target deformed morphing trailing edge shapes. The optimization approach consists of a Genetic Algorithm (GA), an analytical sandwich beam model predicting the mechanical behaviours of the morphing trailing edge and a two-dimensional flow property routine, XFoil (Drela 1989), calculating the pressure loads for aeroelastic effects in the design. The proposed optimization method is applied to the design of the morphing trailing edge. For a series of target morphing profiles characterized using experimental studies, the desired stiffness variations in the honeycomb core have been identified with the developed optimization scheme. The optimization results are further verified using Finite Element Method (FEM) and experiments with a demonstrator. The paper is organised as follows: the morphing trailing edge concept is introduced first and then effects of morphing profiles on the aerodynamic performance are briefly described; the optimization approach is then described including the structural model, the aeroelastic analysis procedure and the optimization formulations followed by the optimization results and discussions. Finally, FEM and experimental studies on a selected optimization result are carried out and results subsequently discussed.

The morphing trailing edge design

Variable stiffness materials have been studied for applications involving morphing structures and offer potential for improved structure performance. The structural efficiency could be significantly increased by selectively tailoring the material stiffness in the morphing structures due to the deformed shape and actuation effort considerations(Ai *et al.,* 2015; Kuder *et al.* 2013). In previous studies by the authors, a novel morphing trailing edge concept was proposed (Ai *et al.,* 2015, 2016a,b)], which consists of three main parts: 1) a carbon fibre reinforced plastic (CFRP) laminate upper skin, 2) a honeycomb core of zero Poisson's ratio (ZPR) with axial variable stiffness and 3) a silicone lower skin. The concept extends

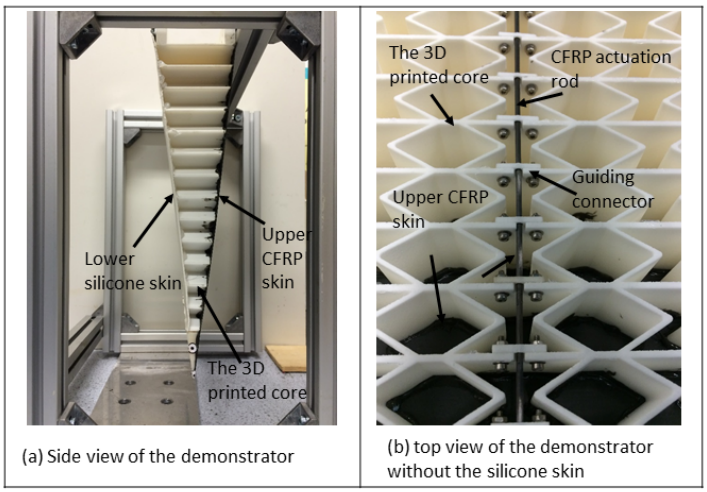

Figure 2. A morphing trailing edge using bending stiffness tailored core

the morphing trailing edge device developed by Daynes *et al.*(2012a; 2012b). As shown in Figure 2, the upper composite skin provides a smooth structural surface and the bending rigidity of the flap and the honeycomb core reinforces the through-thickness stiffness of the morphing trailing edge. The bottom side is covered with silicone for a smooth, weather tight surface. An actuation CFRP push/pull rod is embedded on the bottom side of the core with one end glued to the tip of the morphing trailing edge using epoxy resin. The rod is also constrained using nylon guiding connectors attached to the honeycomb core which only allows the rod to move in and out the flap along the bottom surface and prevents its movement through the honeycomb core thickness direction. A zero Poisson's ratio (ZPR) honeycomb core is used instead of off-the-shelf hexagon honeycomb core to eliminate the unwanted curvature change in the non-morphing direction, in this case, span-wise due to the anticlastic effect (Daynes and Weaver 2012a; Ai *et al.,* 2015). Due to the lack of commercially available ZPR honeycomb core with axial variable stiffness, a cellular solid design (Bubert *et al.,* 2010; Ai *et al.,* 2015) is adopted in this study of which the in-plane stiffness depends on the geometrical parameters. The in-plane stiffness of the ZPR honeycomb core along the trailing edge chord can be effectively changed through varying unit cell wall thickness with limited effects on the through-thickness direction stiffness of the core.

The morphing trailing edge using stiffness tailored honeycomb core can provide large trailing edge deflections, potential reduction of actuation requirements and also the control capability over the deformed shape, *i.e.* the morphing profile. The morphing profiles (see Figure 3) have been found to significantly affect the aerodynamic performance and noise emission of the aerofoils, extending the potential performance design envelope (Ai *et al.,* 2015, 2016b). Following the results from previous studies, a design optimization methodology to identify the required material stiffness variation in the honeycomb core to match the prescribed profile is now proposed and both FEM and experiments are carried out for a specific design case as well to verify the developed optimization approach.

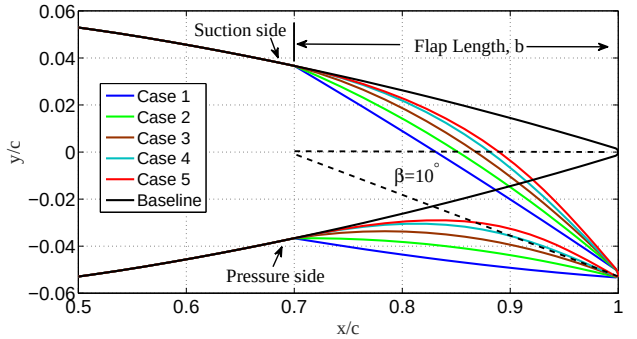

Figure 3. Morphing profiles for a NACA 0012 aerofoil in experimental studies (Ai *et al.,* 2016b): the suction side has a CFRP skin while the pressure side is covered with a silicone sheet.

Variable stiffness honeycomb core design

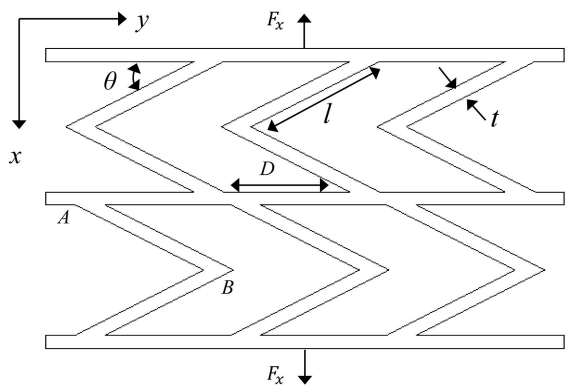

Figure 4. Unit cell geometry definition of the honeycomb core substructure (Ai *et al.,* 2015)

Due to their high anisotropy in mechanical properties, cellular solids and honeycomb core have received significant attention from the morphing research community (Gibson and Ashby 1997; Olympio *et al.,* 2009, 2010; Bubert *et al.,* 2010) and particular interest is given to the zero Poisson's ratio (ZPR) honeycomb core which has no anticlastic effect when subject to bending in one direction. A honeycomb core of zero Poisson's ratio (Bubert *et al.,* 2010) is adopted in this study. The ZPR honeycomb core proposed consists of oblique cell walls and delimitation ribs, as shown in Figure 4. When the honeycomb core is subject to tensile or compressive loads along the x-axis, the oblique cell wall deforms while the deformation of the delimitation ribs is negligible, resulting in intact configuration along y-axis, namely the ZPR phenomenon. As per cellular solids theory (Gibson and Ashby 1997), the in-plane stiffness of the proposed core is expressed as:

$$\frac{E_x}{E_0} = (\frac{t}{l})^3 \frac{\sin\theta}{\frac{D}{l}\cos^2\theta}. \tag{1}$$

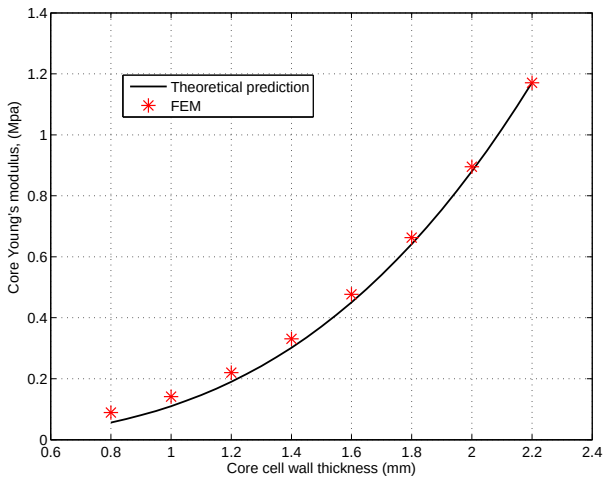

Figure 5. Verification of the analytical in-plane stiffness predictions

The analytical expression of the core's stiffness in Eq 1 is firstly verified using FEM models from Abaqus. Our honeycomb core has a geometry configuration of $\theta = 30°$, $l = 20\ mm$, $D = 25\ mm$ and the oblique cell wall thickness t varies from 0.8 mm to 2.2 mm. The material is a polyamide polymer used for the laser sintering technique and has a Young's modulus of 1650 MPa. Shell elements S4R are adopted and after a mesh convergence analysis, a mesh size of 2 mm and 1 mm are selected for the rib and core cell wall respectively. Figure 5 presents the results from the analytical model and FEM and good agreement has been observed. It is noticed that by changing the thickness of the oblique cell wall of the ZPR honeycomb core the in-plane stiffness can be effectively tailored over a wide range of values.

Design optimization methodology

Selectively changing the honeycomb core's axial stiffness enables reduction of the actuation force and scope for tailoring of morphing profiles, leading to extended lift control and noise mitigation capability. In this section, a design optimization approach is developed using an analytical sandwich beam model of the morphing trailing edge, an aerodynamic routine Xfoil (Ai *et al.,* 2015; Daynes and Weaver 2012b; Previtali *et al.,* 2016) and a GA in the commercial software package Matlab (MATLAB R2013a, The MathWorks Inc., Natick, MA, USA). The aim of the proposed optimization approach is that for a selected morphing profile, it provides the required structural design parameters, *e.g.* the stiffness variation in the honeycomb core that provides the expected deformed shape of the morphing trailing edge, *i.e.* an inverse engineering design method. Note, the prescribed target morphing profiles can be obtained using various

methods including wind tunnel tests and aerodynamic or aeroacoustic optimization design studies, which can be incorporated within the optimization approach proposed herein forming a two-level optimization design methodology (De Gaspari *et al.,* 2011). However, the selection of optimal profiles is beyond the current scope and the previously tested morphing profiles shown in Figure 3 are chosen as the design target profiles in this study.

Structural model

An analytical sandwich beam model has been developed for the design optimization process of the proposed morphing trailing edge (Ai and Weaver 2017). The proposed morphing trailing edge device has a sandwich structure: a composite laminate upper skin, a silicone lower skin and a honeycomb core of axial variable stiffness. As such, a layer-wise sandwich beam model considering the trailing edge geometric taper and the axial stiffness variation in the core (Ai and Weaver 2017) is used in this section.

In the sandwich beam model, the morphing trailing edge of NACA 0012 aerofoil is approximated as a symmetric triangular configuration, providing small modelling error (Daynes and Weaver 2012a,b). The face sheets are modelled as Euler beams and the honeycomb core is modelled using a first order shear deformation theory. With the skin/honeycomb core interface geometric compatibility conditions applied, only three beam state variables are used in the model to fully capture the mechanical behaviour of the sandwich beam: the transverse, extensional and rotational displacements at the centroid of the honeycomb core.

The beam deflections, particularly the transverse deflection of the morphing trailing edge, can be obtained by solving the resulting matrix equations. Note, it has been found that for a cantilever sandwich beam such as a the morphing trailing edge, the linear strain-displacement relations could provide accurate predictions with a significantly reduced computation cost compared to a non-linear beam model (Ai and Weaver 2017) and is adopted for the study in this paper. In order to assess the accuracy of the proposed analytical model, results of the analytical model are compared with those from the static mechanical tests of the morphing flap device developed previously (Daynes and Weaver 2012a,b). For simplification purposes, the CFRP actuation rod is not modelled in detail and only considered as a reinforcement of the bending stiffness of the structure and the actuation forces are applied at the trailing edge. With this simplification, the design scope can be fully focused on the morphing trailing edge itself and also provides the capability of changing the current actuation method if necessary.

As shown in Figure 6, the present model is able to provide a reasonably good approximation of the actuation forces in comparison with mechanical tests. The hysteresis phenomenon shown in the experimental tests is due to the friction between the actuation rod and the core, which is ignored in the current analytical model. The analytical model was reported to accurately calculate the load-displacement response and also to predict the deformed shapes of the trailing edge, with an error less than 2 % (Ai and Weaver 2017). Therefore, the model is selected for the preliminary design optimization of the morphing trailing edge. However, it is of note that there are some nonlinear effects that are not considered in the model, such as the friction between the CFRP rod and the core, the geometric nonlinearity of the rod and the beam under large deformation. As a simplified model, the present formulation provides a good compromise between computational cost and results accuracy. Higher fidelity and therefore more computationally expensive models, typically 3D FEM, may be necessary for the detailed design phase.

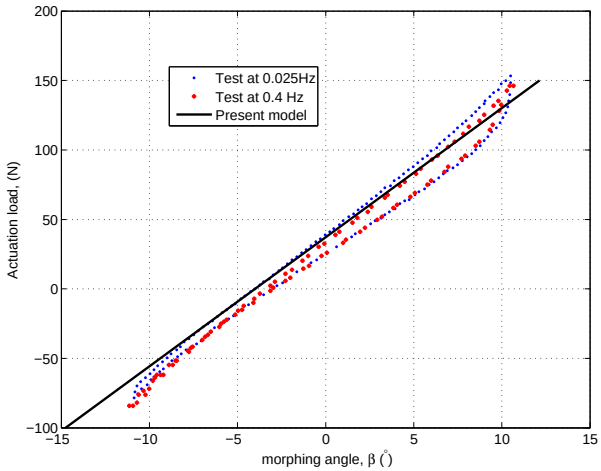

Figure 6. Validation of the present sandwich structural model: Force and morphing angle prediction of a morphing flap by Daynes *et al.* (2012a)

Static aeroelastic analysis

Aerodynamic loads on aerofoils significantly affect the morphing trailing edge's deformation (for both the deformed profile and actuation forces) and hence consideration of fluid/structure coupling effects are essential to obtain a realistic structural design. In this section, a static aeroelastic analysis procedure is developed using an aerodynamic routine Xfoil, a two-dimensional viscous panel model which has been widely used for aerofoil design and fluid/structure coupling analysis (Woods *et al.,* 2015; Daynes and Weaver 2012b). In the aero-structural design optimization procedures, aerodynamic loads are calculated and transferred to the structural model noting that different ways have been used in the literature (De Gaspari *et al.,* 2011):

- The aerodynamic loads are taken as a design requirement and only the target pressure loads are calculated and applied to the structure at each step;
- The aerodynamic loads are considered as design variables, which are calculated and applied to the model at each iteration.

In the first method, one only needs to calculate the pressure distribution once for all of the optimisation process and the aerodynamic loads correspond to the target shape only, which leads to inaccuracy of the pressure loads due to the discrepancy between the optimization solution and the target shape. However, the second method considers the interactive process and pressure loads are calculated at each step until the solution converges. In the current work, the second approach is chosen and the aerodynamic pressure loads are calculated using Xfoil.

In the aeroelastic analysis, as shown in Figure 7, for each iteration the aeroelastic analysis must achieve convergence of the trailing edge deflection for time δ_t, under both actuation force F and pressure loads $p(x)$. The working flow of the proposed aeroelastic analysis procedure is described as follow: firstly, an

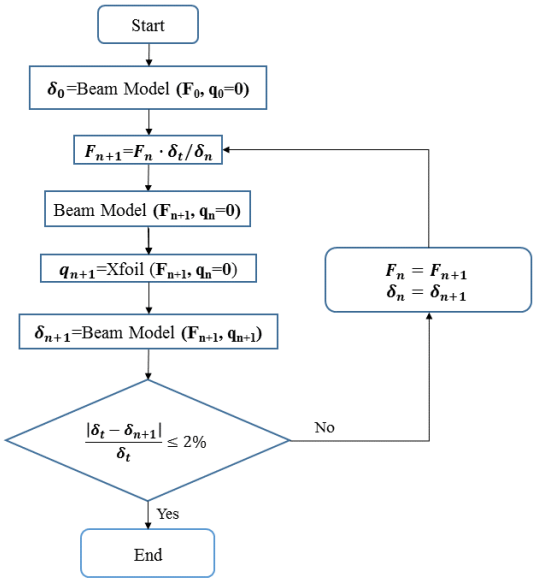

Figure 7. The static aeroelastic analysis procedure

Table 1. Material properties of IM7 prepreg material

Material	$E_{11}(GPa)$	$E_{22}(GPa)$	$G_{12}(GPa)$	$\nu_{12}(-)$	Thickness (mm)
8552/IM7	161	11.4	5.17	0.3	0.133

initial actuation load F_0 is applied and the trailing edge deflection δ_0 is calculated without the pressure load ($q_0 = 0$ MPa) with the beam model (BM). With the initial load and the trailing edge deflection predicted, a new actuation F_{i+1} load can be predicted readily and then the structural deformation can be obtained and interpreted using a MATLAB script for pressure loads calculations with XFoil. Secondly, the output of Xfoil is processed and fitted as a polynomial pressure function of flap length, $p(x)$, combining the pressure loads on both the suction and pressure side of the morphing trailing edge. The pressure load $p(x)$ is then applied to the beam model together with the actuation force F_{i+1} for a new trailing edge deflection, resulting in a new actuation load F_{i+2} and a new trailing edge deformation profile for Xfoil calculations. The second step is repeated until an aeroelastic equilibrium is obtained for the morphing trailing edge. As shown in Figure 7, static aeroelastic equilibrium is achieved by minimising the tip deflection difference between the two adjacent steps until convergence criteria are satisfied.

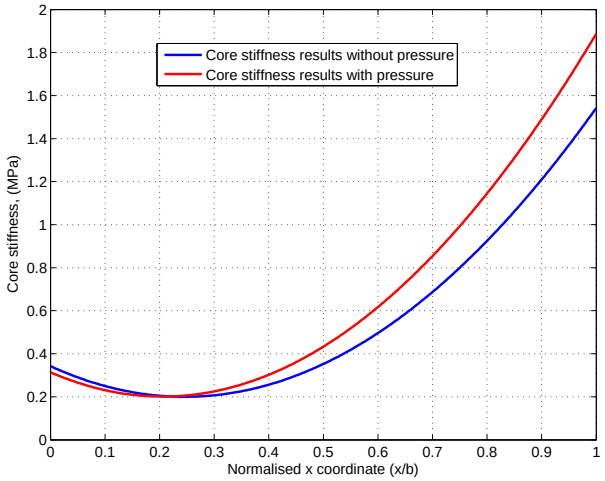

(a) Optimisation results of honseycomb core stiffness variation

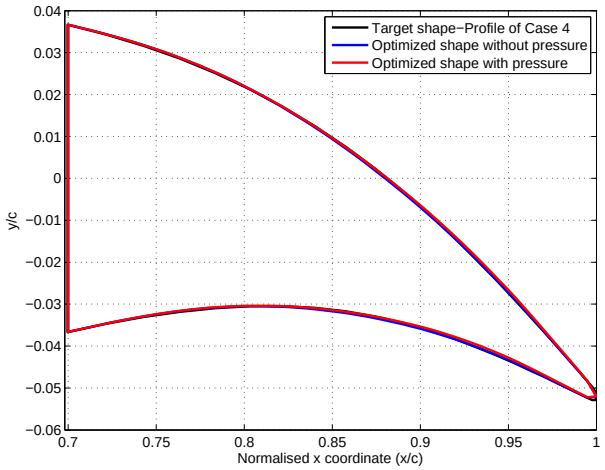

(b) Optimised deformed shape of the morphing trailing edge

Figure 8. Optimization results of the morphed trailing edge with the profile of Case 4: (a) the in-plane Young's modulus of the core ; (b) the deformed shapes of trailing edge with identified core

Optimization formulation

In this section, the design optimization formulation is proposed and described for a morphing trailing edge. A NACA 0012 aerofoil of chord length, c= 1 m, fitted with a morphing trailing edge of 30% chord length is selected for the optimization study. Morphing profiles Case 1-5 presented in Figure. 3 which have been used in our previous aerofoil performance characterization studies (Ai *et al.,* 2016b) are chosen

as the target shape. The morphing trailing edge design length is 300 mm with a cellular core of length b of 270 mm, between 0.7c to 0.97c, and the rest of the trailing edge (30 mm) taken as a rigid tip. The morphing trailing edge design has a width of 250 mm and the root thickness of the honeycomb core is 73 mm and taper angle is 6.94°. The CFRP upper skin is made of IM7/8552 prepreg with a layup of [90/0/90] with 0° along with the chord direction. The IM7/8552 material mechanical properties used in this paper are given in Table 1 and classical laminate theory (Jones 1999) is adopted to calculate the equivalent laminate mechanical properties. The CFRP actuation rod has a diameter of 2 mm, a longitudinal modulus of 152 GPa and a lateral modulus of 10 GPa. The bottom layer is made of silicone with a Young's modulus of 1 MPa. A flow velocity of 30 m/s and an angle of attack of 0° is chosen for the pressure load calculations using Xfoil. The optimization scheme identifies the stiffness distribution parameters in the core, while simultaneously monitoring the actuation force and the effect of the pressure load on the deformation.

Deformation in the thickness direction of the morphing trailing edge is neglected in this analysis and the morphing profiles are defined as the transverse displacement of the beam, $w(x)$. The optimization objective is defined in terms of the least square error (LSE) between the target shape and deformed beam curve at selected flap positions, as shown in Eq 2. Six geometric control points along the morphing trailing edge length are selected, *i.e.* $\frac{x_i}{c} = [0.7, 0.85, 0.93, 0.95, 0.98, 1]$. It is worth noting that the curvature and shape of the morphing trailing edge near the trailing edge play an important role in the noise emission of the aerofoil (Ai *et al.,* 2015) and, as such, more points are selected in this region with larger weight coefficients in the optimization objective. For simplification purposes, the honeycomb core is assumed to have a continuous axial stiffness variation, $E(x)$ and in this paper, a quadratic polynomial type in-plane stiffness variation is chosen, *i.e.* $E(x) = e_0 + e_1 x + e_2 x^2$. In order to develop a physically feasible solution for the trailing edge design, constraints have been set for the core chord wise stiffness variation, which varies from 0.2 MPa to 2 MPa. The optimization formulation includes targets, variables and candidates given as follows:

$$\begin{aligned} Minimize: \quad & LSE = \frac{1}{N}\sum_i^N \sqrt{(w_{t,i} - w_{d,i})^2}, \\ Variables: \quad & \{e_0,\ e_1,\ e_2\}, E(x) = e_0 + e_1 x + e_2 x^2, \\ Subject\ to: \quad & 1)\ E_c(x) \in (0.2, 2), x \in [0, L], \\ & 2)\ e_0 \in [0.2, 2], \\ & 3)\ e_1 \in [-0.5, 0.5], \\ & 4)\ e_2 \in [-0.5, 0.5]. \end{aligned} \tag{2}$$

Due to the non-convex nature of the inverse design problem, a Matlab Neld-Mead optimization algorithm is combined with the GA forming a hybrid optimization scheme (Groh and Weaver 2015). In the hybrid scheme, a GA is first used to search for the region where the optimal solution lies within the whole design space within a small number of typically less than 60 generations and then a Neld-Mead algorithm is used to further search for the optimal solution near the region more efficiently. In the GA, the crossover probability is chosen to be 0.8 and the population size is 20. The mutation children are created using Matlab's Gaussian function. The constraint function, $E_c(x) \in (0.2, 2)$, is implemented by

introducing a penalty constant to the LSE. The design variables are $\{e_0,\ e_1,\ e_2\}$ which determines the in-plane stiffness distribution function of the core and initial ranges are chosen after an initial parametric study to simplify the design process and reduce the computational cost. An objective penalty constant is used in the optimization scheme to further constrain the design space to satisfy $E_c(x) \in (0.2, 2)$, and after a couple of trial studies, was fixed at a value of 10. The design optimization results are discussed in detail in the following section.

Optimization results and discussions

The optimization results are shown in Figures 8 to 9 including the optimised morphing profiles and the identified honeycomb core stiffness distributions for cases with and without aeroelastic effects considered in the design. Good correlation between the target profile shape and the optimised morphing trailing edge profiles is observed for both Case 4 and Case 5, as shown in Figure 8(b) and 9(b). Furthermore, as expected, the aerodynamic loads significantly affects the optimization results and a stiffer core is required to carry the pressure loads, leading to an increase of actuation energy as found in Case 5 in Figure 9(a) while Case 4 presents a reduced stiffness at the root region in the core design with aerodynamic loads compared to that of results without pressure considered. However, it has been found that as the morphing profiles change from Case 5 (the most curved shape featuring a typical bending behaviour) to Case 1 (a typical deflection of hinged flap), it becomes harder for the optimization scheme to converge. Due to the non-convex nature of the problem, the selected results chosen may not be the globally optimal solution. The discrepancy between the target shape and the optimized profiles for design cases with or without the pressure loads applied significantly increases from Case 3 to Case 1. It is believed that as the morphing profiles become less curved (from Case 5 to Case 1), the trailing edge deforms more similarly to a hinged-flap which rotates about an axis at the flap root and presents less bending type structural deformation. To solve this issue, a structural model considering different boundary conditions including non-zero transverse shear deformation at the root of the trailing edge and a wider material property range would be a useful development in future work.

The design optimization process has successfully identified the required material properties for various target shapes under different conditions. The present model provides insights into the coupling between the structural design and the aerofoil aerodynamic performance, enabling a more realistic design to be identified. The design optimization space can be further extended by considering different skin materials, actuation methods and also the topological design of the honeycomb core. In the following sections, a proof-of-concept demonstrator is built and tested to validate the idea of tailoring morphing profiles with a honeycomb core of axial variable stiffness. The optimised honeycomb core design for Case 5 without pressure loads is selected for further studies.

FEM of the morphing trailing edge

From our optimization results, continuous axial stiffness variations in the honeycomb core have been successfully identified for the set target morphing profiles. However, due to the fact that no commercially available cores satisfy the required stiffness variation, rapid prototyping technique (3D printing) is used to manufacture the honeycomb core of axial variable stiffness. In this section, the optimized honeycomb core of axial variable stiffness for Case 5 without pressure loads is selected and re-designed for FEM and experimental studies. The optimized core stiffness of morphing profile Case 5 without pressure is further

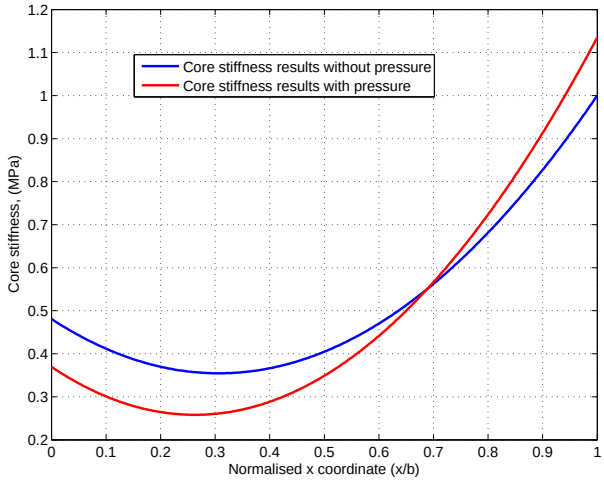

(a) Optimisation results of honseycomb core stiffness variation

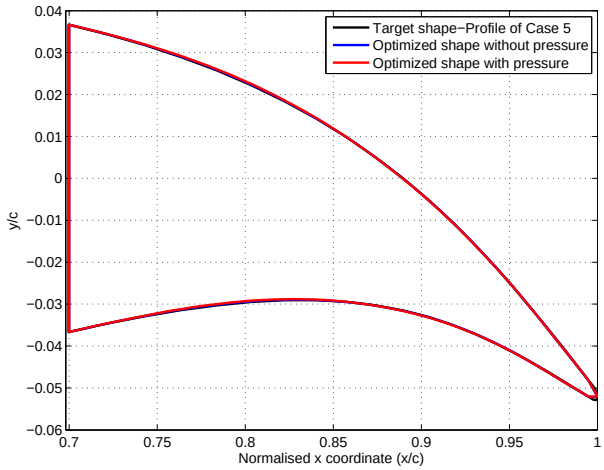

(b) Optimised deformed shape of the morphing trailing edge

Figure 9. Optimization results of the morphed trailing edge with the profile of Case 5: (a) the in-plane Young's modulus of the core ; (b) the deformed shapes of trailing edge with identified core

discretized into thirteen sections along the honeycomb core length (270 mm), as shown in Figure 10 and the cell wall thickness is then predicted using Eq 1.

With the honeycomb core of variable oblique cell wall thickness designed (see Figure 10), a three-dimensional FEM of the morphing trailing edge featuring the ZRP honeycomb core of tailored in-plane stiffness designed is prepared using Abaqus to validate the feasibility of the proposed methodology using discretized core stiffness distribution that realizes the optimization results.

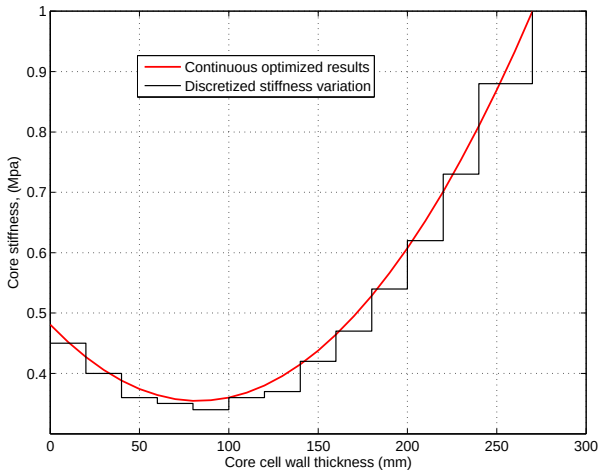

Figure 10. The discretized core stiffness variation for optimization results of morphing profile Case 5

As shown in Figure 11, the FEM was prepared using S4R shell elements and the upper skin uses the equivalent homogeneous material property of the laminate obtained using classical laminate theory. Polyamide material property with a Young's modulus of 1650 MPa and Poisson's ratio of 0.3 is used for the honeycomb core. The honeycomb core has the same in-plane geometrical parameters defined in the last section. The oblique cell wall thickness is predicted through Eq 1 and assigned to the cell wall sections in the model. Both the ZPR honeycomb core and skins are modelled with S4R shell elements while the actuation rod is modelled using beam elements B31. After a mesh convergence study, a mesh seed of 2 mm is used for the core and skin while the rod has a mesh seed of 4 mm. The actuation CFRP rod is restrained to the bottom surface of the core using coupling constraints which only allows the rod move in and out of the core and prevent its movement in the core's thickness direction (see the bottom view of Figure 11). The actuation rod is tied at one end to the trailing edge at the centroid of the last delimitation rib and the actuation forces are applied at the free end of the actuation rod. A clamped boundary condition is applied at the rear end of the morphing trailing edge and displacement at the trailing edge is monitored as well as the deformed shape of the top skin. Nonlinear geometrical effects due to the possible large morphing trailing edge displacements are also considered in the current FEM analysis.

Manufacture and test of the demonstrator

A prototype hardware morphing trailing edge device was built as a proof-of-concept demonstrator. The honeycomb core designed is manufactured using a laser sintering technique (see Figure 12) and the raw material is polyamide polymer. As shown in Figure 12, the honeycomb core prototype has three parts: the trailing edge tip of 40 mm in length, the morphing honeycomb core section of 260 mm in length and the rear spars used for attachment with other structural components. The thickness of the core at the root is 73 mm and gradually decreases towards the trailing edge. The thickness of the oblique

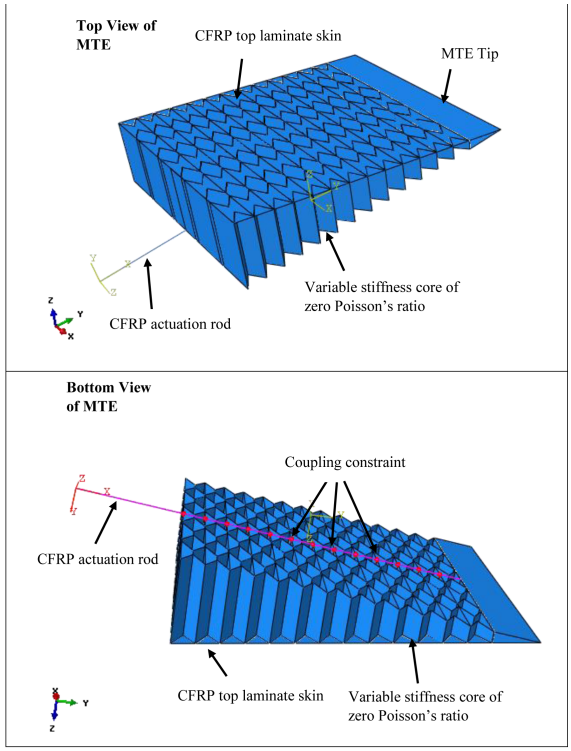

Figure 11. Three-dimensional FEM model of the morphing trailing edge (bottom skin is not shown for purposes of clarity)

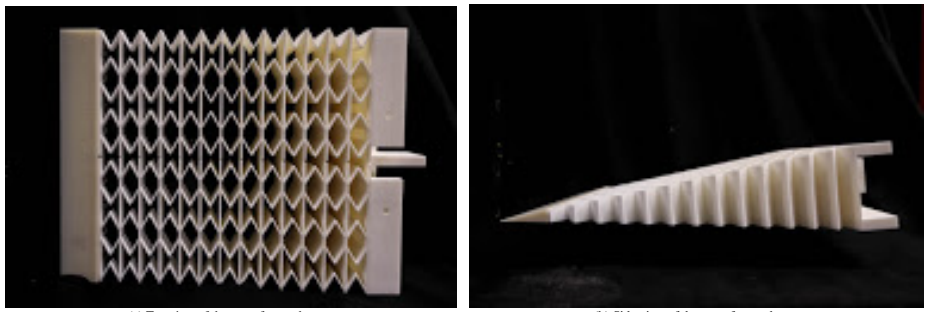

(a) Top view of the manufactured core

(b) Side view of the manufactured core

Figure 12. Laser sintered polyamide honeycomb core with zero Poisson's ratio

cell walls are calculated using Eq 1 and the stiffness distribution defined in Figure 10 and the in-plane geometry parameters used are: $\theta = 30°$, $l = 20\ mm$, $D = 25\ mm$ (see Figure 4). The top skin is made

of IM7/8552 CFRP prepreg and has a layup of [90/0/90] with 0° along the chord direction which further increases the anisotropy of the morphing trailing edge. The CFRP laminate skin has a thickness of 0.4 mm. The bottom skin is made from silicone sheet which is both durable and soft. The CFRP actuation rod is selected with one end tied to the centroid of the trailing edge using helical coil and a mechanical linkage is attached to another end for applying the actuation forces. The actuation rod is constrained to the bottom surface of the honeycomb core with 13 guiding connectors which are made of the same material as the core using 3D printing and fixed at the mid-span position of the delimiter cell wall of the core. The rod penetrates through the guiding connectors and can only slide in/out the core with the movement along the thickness of the core prohibited. All the pieces are interchangeable including the CFRP actuation rod, the honeycomb core and the guiding connectors, which de-risks the success of the morphing trailing edge device and allows for a rapid change of damaged structural components.

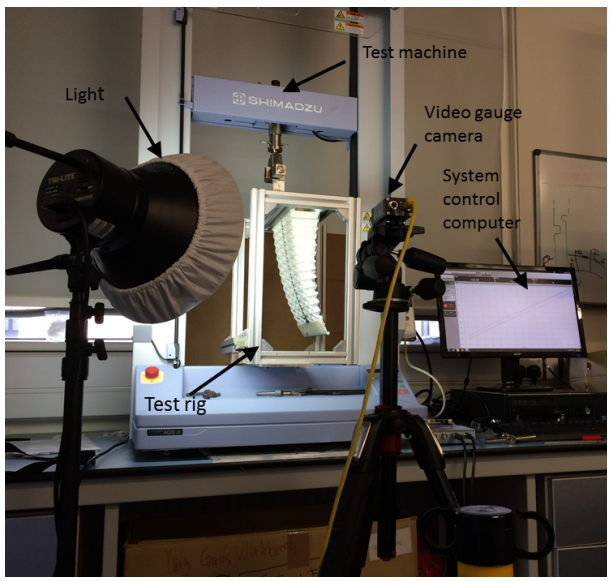

Figure 13. Static mechanical test set-up (in this test, the morphing flap has only the upper CFRP skin attached.)

The morphing trailing edge demonstrator is subsequently tested for actuation requirements and particularly the morphing profiles. The static mechanical tests set-up is shown in Figure 13 and a test rig was prepared to support the demonstrator and the morphing trailing edge was fixed to the top spars of the rig for the clamped boundary condition. The CFRP actuation rod was connected to the 1 kN load cell of a Schimadzu universal/tensile testing machine. In the tests, stroke control is used which applies displacements to the actuation rod and the corresponding reaction load is monitored. An Imetrum video gauge system (see Figure 13) is used to monitor the real-time deformed shape of the morphing trailing edge simultaneously with the load/stroke control system. Sixteen targets were selected along the edge of the top skin from the root to the trailing edge. The video was recorded together with the static mechanical tests and processed to calculate the transverse displacement of the selected monitoring targets.

After a comprehensive parametric study with testing under different load types *i.e.* single, cyclic and increasing test speeds, the morphing trailing edge deformation angle β is found to be linearly correlated to the stroke δ applied and can be expressed as : $\beta = e_0 \times \delta$ and in this case e_0 was found to be a constant of 0.7 $^\circ/mm$. This phenomenon was also observed in previous studies (Daynes and Weaver 2012a,b). Different test speeds have been selected and converted into deformation angle speeds.

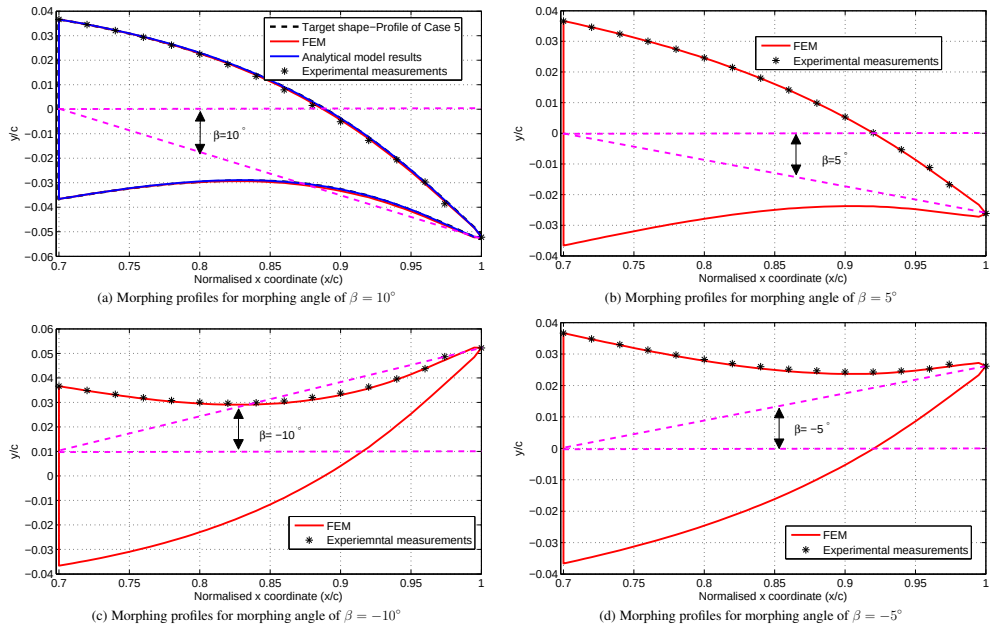

(a) Morphing profiles for morphing angle of $\beta = 10^\circ$

(b) Morphing profiles for morphing angle of $\beta = 5^\circ$

(c) Morphing profiles for morphing angle of $\beta = -10^\circ$

(d) Morphing profiles for morphing angle of $\beta = -5^\circ$

Figure 14. Deformed shapes of the morphing trailing edges obtained using FEM, the analytical model and tests for different morphing angles : (a), $\beta = 10^\circ$; (b), $\beta = 5^\circ$; (c), $\beta = -10^\circ$ and (d), $\beta = -5^\circ$

Figures 14 and 15 present results of the static mechanical tests in comparison with the analytical model and FEM for the morphing profiles and the load-trailing edge morphing angle curves respectively. It is worth noting that the analytical results provided are for the optimized results of Case 5 without pressure loads considered which has a continuous stiffness variation in the honeycomb core identified by the optimization approach. Both the FEM and experiment results are obtained with the discretized honeycomb core stiffness (see Figure 4). As shown in Figure 14, good agreement between the morphing profiles of FEM and the demonstrator is found and they all match well with the target deformed shape of morphing profiles Case 5 in Figure 3 for a morphing angle of $\beta = 10^\circ$ at the trailing edge. These confirm the feasibility of the developed optimization approach as well as the proposed method for building the morphing trailing edge using honeycomb core of discetized axial variable stiffness. Furthermore, besides the target morphing profiles of Case 5 (see Figure 3), measured deformed shapes of the morphing trailing edge for another three different morphing angles of $\beta = 5^\circ$, -5° and -10° (positive morphing angles are defined as deflections towards the pressure side of the aerofoil) are also compared with FEM. As

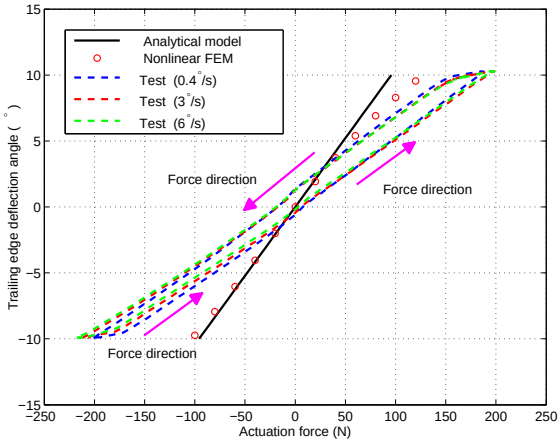

Figure 15. The morphing trailing edge deflection angle–the actuation load plot

shown in Figure 14(b), 14(c) and 14(d), the three dimensional FEM provides accurate predictions over the morphing profiles compared with the experimental measurements.

Significant discrepancies, however, are observed in the actuation requirements predicted by the analytical model, FEM and tests, as shown in Figure 15, especially for the positive morphing angle range, *i.e.* the downwards deflection of the morphing flap. The demonstrator was tested successfully with a speed of up to 6 $^{\circ}/s$. The test results show that the actuation speed does not significantly affect the actuation forces. Compared to the experimental results, the actuation requirement predicted using FEM correlate well with the analytical model as shown in Figure 15. Note, the discrepancy between the FEM and the analytical model for positive morphing angles (corresponding to deflections towards the pressure side of the trailing edge) is due to the nonlinear effects present in the actuation CFRP rod subject to tension loads. It is believed that the nonlinear deformation modes of the rod under tension and bending as well as the contact effects between the rod and the core's cell wall are the two main causes for the discrepancies arising from the analytical model. These nonlinear effects are not modelled in the analytical model and can be improved with a simple empirical factor or a more accurate structural model of the morphing trailing edge including the actuation rod. The demonstrator has significantly increased actuation forces and it is believed to be due to the friction between the actuation rod and the polyamide guiding connectors.

Both numerical and experimental studies have confirmed the feasibility of the developed optimization approach to identify the stiffness variation in the honeycomb core for a set target profile. The proposed method of using discretized honeycomb core stiffness to realize the continuous stiffness variation identified with the design optimization is also successfully proved using FEM and static mechanical tests.

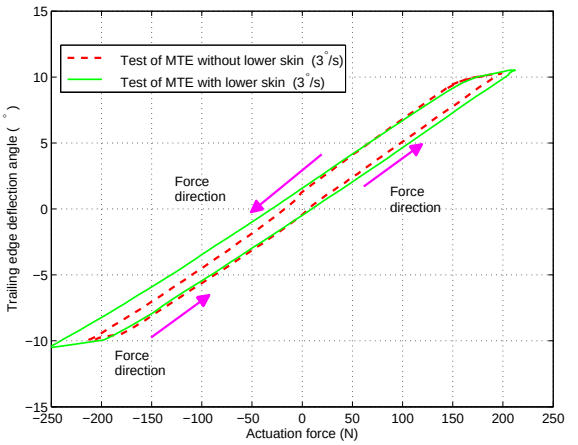

Figure 16. Effects of the pretensioned lower silicone skin on the actuation energy requirement

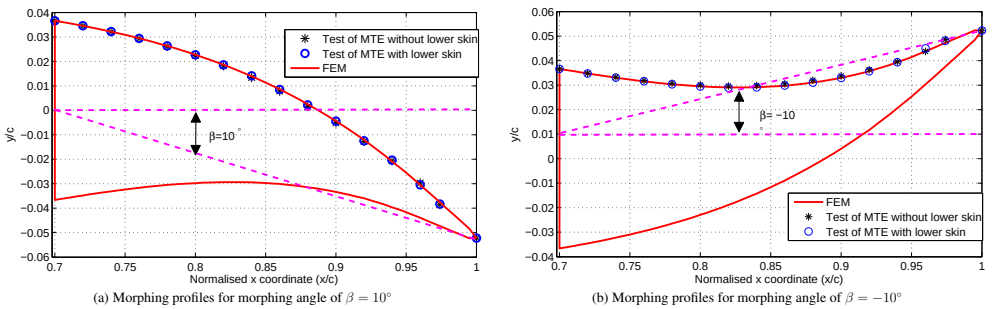

(a) Morphing profiles for morphing angle of $\beta = 10°$

(b) Morphing profiles for morphing angle of $\beta = -10°$

Figure 17. Effects of the pretensioned lower silicone skin on the deformed shapes of the morphing trailing edge: (a), $\beta = 10°$; (b) $\beta = -10°$.

Effects of the pretensioned lower silicone skin

The main scope of the paper is devoted to the design of the stiffness tailored honeycomb core while the upper/lower skins design are left unexplored. The asymmetric sandwich structure of the proposed morphing trailing edge requires a stiff skin on one side and a flexible skin on the other side. In this paper, a CFRP laminate and a silicone sheet have been used as the upper and lower skins respectively. Optimization studies on the CFRP upper skin could be carried out to further extend the material property range and structural design space while a few options are available for the flexible lower skin including elastomer silicones and elastomeric matrix composites (Falken *et al.,* 2016) .

In the proposed morphing trailing edge design, the chosen silicone is flexible and durable and has a low Young's modulus of 1.4 MPa and was pretensioned before being applied to the structure to mitigate

the deleterious effect of wrinkles on aerodynamic performance during trailing edge deflection towards the pressure side of the aerofoil. Pretension or prestress has been considered previously in morphing structures design as an efficient and effective way of material stiffness tailoring (Daynes and Weaver 2013) and also has significant effects on the neutral axis of the structure under loading. Experimental studies have been carried out to characterize the effects of the pretensioned lower silicone skin on the deformed shape and the actuation energy requirement, as shown in Figure 16 and 17 respectively. The actuation forces of the morphing trailing edge are significantly affected by the lower skin although it has low stiffness and most of the changes are observed in the trailing edge deflection angles β of -10° 0°, *i.e.* the trailing edge deflection towards the pressure side of the aerofoil, as shown in Figure 16. This is caused by the tensile stress in the silicone skin which is subject to extension for negative morphing angles. However, for the trailing edge deflection towards the suction side, the silicone is subject to reduced tension due to the pretension effects and in the tests no wrinkles in the lower skin were observed until a moderately high morphing angle β of 8°. Interestingly, no significant changes to the deformed shape of the morphing trailing edge are induced by the lower skin (see Figure 17). The pretensioned silicone skin also leads to a slight retracting deflection of the morphing trailing edge and indicates that for a more realistic structural design with stiffer and thicker silicone materials or elastomeric matrix composites (Falken *et al.,* 2016) these effects should be addressed and also could be exploited to tailor the structural stiffness and the neutral position of the axis.

Conclusion

Morphing technologies including new concepts, smart materials and novel actuation methods have received growing interest due to the drive for high performance control surfaces in aeroplane wings and wind turbine blades. Using spatially variable stiffness materials enables control over the actuation requirements and the deformed shapes of the morphing structure. The morphing trailing edge design using a 3D printed honeycomb core of axial variable stiffness developed herein and the associated design methodology including mechanical tests represent a promising concept for future development of intelligently responsive control surfaces.

In the current study, a design optimization methodology has been developed for a morphing trailing edge design using a zero Poisson's ratio honeycomb core of axial variable in-plane stiffness. The optimization approach couples a GA for optimization, an analytical sandwich beam model and an aerodynamic routine, Xfoil for aeroelastic analyses. Using the developed optimization approach, material stiffness variations *e.g.* the honeycomb core stiffness distribution can be inversely identified by meeting the requirements of a set target deformed shape of the morphing structure. Design optimization studies were then carried out for the morphing trailing edge with a series of experimentally characterized morphing profiles. The model successfully provides the optimised honeycomb core stiffness variations for different target profiles. It has been found that aeroelastic effects significantly affect the structural design and should be taken into consideration for obtaining a realistic, viable solution. However, for morphing profiles which feature less bending deformation in the structure, there are noticeable differences between target shapes and optimized results, which is believed to be due to the limited mechanical property range considered.

Verifications of the proposed optimization methodology are carried out through FEM and experimental studies supported by a demonstrator designed for the honeycomb core stiffness that was identified for a

chosen target morphing profile without pressure loads considered. Due to lack of commercially available honeycomb core that satisfies the required stiffness variation, the rapid prototype technique was used to manufacture the honeycomb core. In order to facilitate the 3D printing method, a honeycomb core design consisting of oblique cell walls and horizontal delimitation ribs is adopted to meet requirements of zero Poisson's ratio and a simplified discretized step-wise stiffness variation was achieved through varying the oblique cell wall thickness. Good agreement was observed for the morphing profiles between experimental measurements, FEM and the optimization model. Both FEM and experimental studies confirm the feasibility of the inverse optimization approach that was developed to successfully identify targeted stiffness parameters. Due to the simplicity of the analytical sandwich beam model, discrepancies were observed for the actuation requirements predicted by the analytical model, FEM and the mechanical test results, which is due to the friction between the actuation rod and the honeycomb core and the nonlinearity in the CFRP actuation rod. Furthermore, due to the laser sintering machine capability, dimensional differences between the designed honeycomb core cell wall thickness and the manufactured one are also observed, which may also contribute to the difference in the actuation energy requirements which could be reduced subsequently using machines of greater accuracy.

As expected, the upper composite skin and the honeycomb core predominantly contribute to the stiffness of the morphing trailing edge and dominate the mechanical responses including the actuation forces requirements and deformation. The pretensioned lower silicone skin significantly changes the actuation forces of the flap in the negative morphing angle range and does not have a significant effect on the deformation shape of the flap. The CFRP actuation rod also contributes to the system stiffness and its light-weight nature satisfies the weight considerations of the morphing structure. However, it is envisaged that a powerful servomotor will cause significant weight penalty to the system.

In future studies, the dynamic response of the manufactured morphing trailing edge and aeroelastic tests are necessary to further characterise performance. Fatigue tests could be carried out to identify possible failure modes and breaking points. Furthermore, in the current morphing trailing edge design, the bottom skin used is a soft and durable silicone sheet and could be replaced with elastomeric matrix composite materials where the matrix dominated direction aligns with the morphing trailing edge chord, and in doing so further increase the load carrying ability of the morphing trailing edge with only minor effects on the actuation requirements.

Acknowledgements

This work was supported by the Engineering and Physical Sciences Research Council through the EPSRC Centre for Doctoral Training in Advanced Composites for Innovation and Science [grant number EP/G036772/1]. QA would like to acknowledge the China Scholarship Council for support. The third author (MA) would like to acknowledge the financial support of the Royal Academy of Engineering.

References

Ai, Q., Azarpeyvand, M., Lachenal, X., Weaver, P. 2015. Aerodynamic and Aeroacoustic Performance of Airfoils Using Morphing Structures, *Wind Energy*, Vol. 19(7), pp: 1325-1339. DOI: 10.1002/we.1900.

Ai, Q., Weaver, P., Azarpeyvand, M. 2016a. Design Optimization of a Morphing Flap Device Using Variable Stiffness Materials, *24th AIAA/AHS Adaptive Structures Conference, AIAA SciTech*, AIAA 2016-0816, San Diego, California, USA. DOI: 10.2514/6.2016-0816.

Ai, Q., Kamliya Jawahr, H., Azarpeyvand, M. 2016b. Experimental Investigation of Aerodynamic Performance of Airfoils Fitted with Morphing Trailing Edges, *54th AIAA Aerospace Sciences Meeting, AIAA SciTech*,AIAA 2016-1563, San Diego, California, USA.DOI: 10.2514/6.2016-1563.

Ai, Q., Weaver, M.P. 2017. Simplified Analytical Model for Tapered Sandwich Beams Using Variable Stiffness Materials. *Journal of Sandwich Structures and Materials*, Vol.19(1). DOI:10.1177/1099636215619775.

Bae, JS., Kyong, NH., Seigler, T., Inman, J. 2005. Aeroelastic Considerations on Shape Control of an Adaptive Wing, *Journal of Intelligent Material Systems and Structures*, Vol. 16, pp:1051-1056, Doi:10.1177/1045389X05059965.

Barbarino, S., Bilgen, O., Aja, R.M., Frishwell, M.I., Inman, D.J. 2011. A Review of Morphing Aircraft, *Journal of Intelligent Material Systems and Structures*, Vol. 22(9), pp:823-877, DOI: 10.1177/1045389X11414084.

Bartley-Cho, JD., Wang, DP., Martin, CA., Kudva, JN., West, MN. 2004. Development of high-rate, adaptive trailing edge control surface to the smart wing phase 2 wind tunnel model. *Journal of Intelligent Material Systems and Structures*, Vol. 15, pp: 279-291. DOI:10.1177/1045389X04042798.

Bubert, EA., Woods, B KS., Lee, K., Kothera, CS., Wereley, NM. 2010. Design and fabrication of a passive 1D morphing aircraft skin. *Journal of Intelligent Material Systems and Structures*, Vol. 21, pp:1699-1717. DOI:10.1177/1045389X10378777.

Campanile, L.F., Sachau, D. 2000. The Belt-Rib Concept: A Structronic Approach to Variable Camber, *Journal of Intelligent Material Systems and Structures*, Vol. 11, No. 3, pp: 215-224, doi: 10.1106/6H4B-HBW3-VDJ8-NB8A.

Campanile, L.F., Anders, S. 2004. Aerodynamic and Aeroelastic Amplification in Adaptive Belt-rib Airfoils, *Aerospace Science and Technology*, Vol. 9, pp:55-63, doi:10.1016/j.ast.2004.07.007.

Campanile LF.2007. *Adaptive Structures: Engineering Applications* (Wagg D, Bond IP, Weaver PM, Friswell MI, eds). Wiley:Chichester, Chapter 4: Lightweight Shape-adaptable Airfoils: A New Challenge for an Old Dream.

Chopra, I. 2002. Review of state of art of smart structures and integrated systems. *AIAA Journal*, Vol. 40, pp:2145-2187. DOI: 10.2514/2.1561.

Daynes, S., Weaver, P. 2012a. A morphing trailing edge device for a wind turbine. *Journal of Intelligent Material Systems and Structures*,Vol. 23, pp: 691-701. DOI:10.1177/1045389X12438622.

Daynes, S., Weaver, P. 2012b. Design and testing of a deformable wind turbine blade control surface. *Smart Materials and Structures*, Vol. 21, pp:105019-105029. DOI:10.1088/0964-1726/21/10/105019.

Daynes, S., Weaver, P. 2013. Stiffness Tailoring Using Prestress in Adaptive Composite Structures, *Composite Structures*, Vol. 106, pp:282-287. DOI:10.1016/j.compstruct.2013.05.059.

Diaconu, C.G., Weaver, P, Mattioni, F. 2008. Concepts for morphing airfoil sections usin gbi-stable laminated composite structures, *Thin-walled Structures*, Vol. 46(6), pp:689-701. http://dx.doi.org/10.1016/j.tws.2007.11.002.

Drela, M. 1989. XFOIL: an analysis and design system for low Reynolds number airfoils. *Lecture Notes in Engineering*, Vol. 54, Chapter: Low Reynolds number aerodynamics, pp:1-12.

De Gaspari, A., Ricci, S. 2011. A two-level Approach for the Optimal Design of Morphing Wings based On Compliant Structures, *Journal of Intelligent Material Systems and Structures*, Vol. 22, pp: 1091-1111, DOI:10.1177/1045389X11409081.

Dobrzynski, W. 2010. Alomost 40 Years of Airframe Noise Research: What did We Achieve?. *Journal of Aircraft*, Vol. 47(20), pp:353-367. Doi: 10.2514/1.44457.

Falken, A., Steeger, S., Heintze, O. 2016. From Development of Multi-material Skins to Morphing Flight Hardware Production, *the 24th AIAA/AHS Adaptive Structures Conference*, AIAA 2016-0318, AIAA SciTech, 4th-8th Jan,

2016, San Diego, California, USA.

Fischer, M., Friedel, H., Holthusen, H., Golling, B., Emunds, R. 2006. Low Noise Design Trends Derived from Wind Tunnel Testing on Advanced High-lift Device, *12th AIAA/CEAS Aeroacoustics Conference (27th AIAA Aeroacoustics Conference)*, Paper No. AIAA 2006-2562, Cambridge, Massachusetts. DOI: 10.2514/6.2006-2562.

Gibson, LJ., Ashby, MF. 1997. *Cellular Solids: structure and properties*, 2nd edn. Cambridge University Press:New York.

Groh, R.M.J., Weaver, P. 2015. Mass Optimization of Variable Angle Tow, Variable Thickness Panels with Static Failure and Buckling Constraint, *AIAA SciTech Forum, 56th AIAA/ASCE/AHS/ASC Structures, Structural Dynamics and Materials Conference*, 5-9 January 2015. Kissimmee, Florida, USA.

Jones RM. 1999. *Mechanics of composite materials* 2nd edn; Taylor and Francis:Philadelphia, 190-202.

Kuder, I.K., Arrieta, A.F., Raither, W.E., Ermanni, P. 2013. Variable Stiffness Material and Structural Concepts for Morphing Applications, *Progress in Aerospace Sciences*, Vol. 63, pp: 33-55.

Kuder, I.K., Arrieta,A.F., Rist, M., Ermanni, P. 2016. Aeroelastic Response of a Selectively Compliant Morphing Aerofoil Featuring Integrated Variable Stiffness Bi-stable Laminates, *Journal of Intelligent Material Systems and Structures*, Vol. 27(14), pp: 1949-1966.DOI: 10.1177/1045389X15620038.

Kuder, I.K., Fasel, U., Ermanni, P., Arrieta, A.F. 2016. Concurrent Design of a Morphing Aerofoil with Variable Stiffness Bi-stable Laminates, *Smart Materials and Structures*, No.25(11), p. 115001(16pp). doi:10.1088/0964-1726/25/11/115001.

Lachenal, X., Daynes, S., Weaver, P. 2013. Review of morphing concepts and materials for wind turbine blade applications. *Wind Energy*, Vol. 16, pp: 283-307. DOI: 10.1002/we.531.

Molinari, G., Quack, M., Dmitriev, V., Morari., Jenny, P., Ermanni. 2011. Aero-Structural Optimization of Morphing Airfoils for Adaptive Wings, *Journal of Intelligent Material Systems and Structures*, Vol. 22(10), pp:1075-1089, DOI: 10.1177/1045389X11414089.

Molinari, G., Quack, M., Arrieta, A.F., Morari, M., Ermanni, P. 2015. Design, Realization and Structural Testing of a Compliant Adaptable Wing, textitSmart Materials and Structures, Vol. 24, No. 10, p 105027 (20pp). doi:10.1088/0964-1726/24/10/105027.

Molinari, G., Arrieta, A.F., Guillaume, F., Ermanni, P. 2016. Aerostructural Performance of Distributed Compliance Morphing Wings: Wind Tunnel and Flight Testing, *AIAA Journal*, Vol.54(12). pp;3859-3871, DOI: //dx.doi.org/10.2514/1.J055073

Olympio, KR., Gandhi, F. 2009. Flexible skins for morphing aircraft using cellular honeycomb cores.*Journal of Intelligent Material Systems and Structures*,Vol. 21, pp:1719-1735. DOI:10.1177/1045389X09350331.

Olympio, KR., Gandhi, F. 2010. Zero Poisson's ratio cellular honeycombs for flex skins undergoing one-dimensional morphing. *Journal of Intelligent Material Systems and Structures*, Vol. 21, pp:1737-1753. DOI: 10.1177/1045389X09355664.

Panesar, A.S., Weaver, P.M. 2012. Optimization of Blended Bistable Laminates for a Morphing Flap, *Composite Structures* , Vol. 94, No. 10, pp:3092-3105, doi:10.1016/j.compstruct.2012.05.007.

Previtali, F., Molinari, G., Arrieta, A.F., Guillaume, M., Ermanni. 2016. Design and Experimental Characterisation of a Morphing Wing with Enhanced Corrugated Wing, *Journal of Intelligent Material Systems and Structures*, Vol. 27(2), pp:278-292, DOI:10.1177/1045389X15595296.

Raither, W., Furger, E., Zundel, M., Bergamini,., Ermanni, P. 2014. Variable-stiffness Skin Concept for Camber-morphing Airfoil, *Journal of Intelligent Material Systems and Structures*, doi: 10.1177/1045389X14546780.

Reckzel, D. 2003. Aerodynamic Design of the High-lift-wing for a Megaliner Aircraft, *Aerospace Science and Technology*, Vol. 7, pp 107-119. doi:10.1016/S1270-9638(02)00002-0.

Shaw, A.D., Dayyani, I., Friswell, M.I. 2015. Optimization of Composite Corrugated Skins for Buckling in Morphing Aircraft, *Composite Structures*, Vol. 119, pp:227-237. doi:10.1016/j.compstruct.2014.09.001.

Takahashi, H.,Yokozeki, T., Hirano,Y. 2016. Development of Variable Camber Wing with Morphing Leading and Trailing Sections using Corrugated Structure, *Journal of Intelligent Material Systems and Structures*,first published online, Doi:10.1177/1045389X16642298.

Thuwis, G.A.A., Abdalla, M.M., Gurdal, Z. 2010. Optimization of a Variable-stiffness Skin for Morphing High-lift Devices, *Smart Materials and Structures*, Vol. 19, No. 12, pp: 124010(10pp), Doi:10.1088/0964-1726/19/12/124010.

Yokozeki, T., Sugiura,A., Hirano,Y. 2014. Development of Variable Camber Morphing Airfoil Using Corrugated Structure,*Journal of Aircraft*, Vol. 51, NO. 3, pp:1023-1029. DOI: 10.2514/1.C032573.

Thill, C., Etches, J., Bond, I., Potter, K., Weaver, P. 2008. Morphing skins, *The Aeronautical Journal* , Vol. 112, pp:117-139.

Thill, C., Etches, J., Bond, I., Potter, K., Weaver, P. 2010. Composites Corrugated Structures for Morphing Wing Skin Applications, *Smart Materials and Structures* , Vol. 19(12), pp:124009.

Weisshaar, T. 2013. Morphing Aircraft Systems: Historical Perspectives and Future Challenges, *Journal of Aircraft*, Vol.50(2), pp:337- 353, DOI: 10.2514/1.C031456.

Woods, B. KS., Bilgen, O., Friswell, M. 2014. Wind Tunnel Testing of the Fish Bone Active Camber Morphing Concept, *Journal of Intelligent Material Systems and Structures*,Vol. 25(7), pp: 772-785, DOI: 10.1177/1045389X14521700.

Woods, B.K.S., Dayyani, I., Frishwell, M.I. 2015. Fluid/Structure-Interaction Analysis of the Fish-Bone-Active-Camber Morphing Concept, *Journal of Aircraft*, Vol. 52,NO. 1,pp:307-319.doi: 10.2514/1.C032725.